

The development of monocyclic pyrazolone based cytokine synthesis inhibitors

Adam Golebiowski,* Jennifer A. Townes, Matthew J. Laufersweiler, Todd A. Brugel, Michael P. Clark, Cynthia M. Clark, Jane F. Djung, Steven K. Laughlin, Mark P. Sabat, Roger G. Bookland, John C. VanRens, Biswanath De, Lily C. Hsieh, Michael J. Janusz, Richard L. Walter, Mark E. Webster and Marlene J. Mekel

Procter and Gamble Pharmaceuticals, Health Care Research Center, 8700 Mason-Montgomery Rd, Mason, OH 45040, USA

Received 3 December 2004; revised 1 March 2005; accepted 3 March 2005

Abstract—4-Aryl-5-pyrimidyl based cytokine synthesis inhibitors that contain a novel monocyclic, pyrazolone heterocyclic core are described. Many of these inhibitors showed low nanomolar activity against LPS-induced TNF- α production. One of the compounds (**6e**) was found to be efficacious in the rat iodoacetate (RIA) in vivo model of osteoarthritis. The X-ray crystal structure of a pyrazolone inhibitor cocrystallized with mutated p38 (mp38) is presented.

© 2005 Elsevier Ltd. All rights reserved.

Numerous efforts in anti-inflammation research have been focused on the development of small molecule inhibitors of cytokine release. The overexpression of cytokines, such as TNF- α and IL-1 β , has been implicated in a number of serious inflammatory disorders. Consequently, agents that inhibit the production of TNF- α can decrease levels of these proinflammatory cytokines,¹ and thereby reduce inflammation and prevent further tissue destruction in diseases such as rheumatoid arthritis (RA),² osteoarthritis (OA),³ and Crohn's disease.

We are interested in the efficacy of our inhibitors against the overall cascade that leads to TNF- α production and have identified p38 MAP kinase as one of the critical targets of inhibition. However, considering that many other kinases (e.g., JNK, MAPKAPK2) participate in the signaling cascade leading to TNF- α synthesis induction and that p38 kinase itself exists in several conformational states (inactive and active conformations being the major ones) we decided to use a whole cell assay (inhibition of TNF- α release from lipopolysaccharide (LPS) induced THP-1 cells) as our primary screening tool.

Many other small molecule TNF- α production inhibitors have been reported containing a common 4-aryl-5-pyrimidinyl based motif fused to a 5- or 6-membered heterocyclic core. SB203580¹ (Fig. 1) represents a prototypical pyridyl imidazole-based inhibitor, although numerous structural classes, for example, pyrroles, pyrimidines, pyridines, pyrimidones, indoles, heteroindoles, ureas, and various fused bicyclic heterocycles containing a variety of functionality have been reported to inhibit cytokine activity.⁴

In our previous paper, we reported the development of a class of triazole based cytokine inhibitors (e.g., **1**; Fig. 1).⁵ Researchers from Merck reported studies on pyrroles and other heterocycles as inhibitors of p38 kinase.⁶ Two monocyclic pyrazolones were presented (e.g., **2**; Fig. 1) with good p38 α -kinase inhibition, but weak whole cell assay activities. We speculated that alkyl substitution of both pyrazolone ring nitrogen atoms could facilitate cell membrane permeability and improve cellular cytokine synthesis inhibition profile. This led to the development of mono-, bi-, and tricyclic pyrazolones as an emerging, leading series in our project.^{7–9} Many compounds in these scaffolds exhibited good to excellent activities in the THP-1 cell-based assay, inhibiting the production of TNF- α with IC₅₀s in the low nanomolar range. Herein we wish to report the synthesis and structure–activity relationships for the series of monocyclic

Keywords: Cytokine synthesis inhibitors; p38 kinase.

* Corresponding author. Tel.: +1 513 622 3802; fax: +1 513 622 3681; e-mail: golebiowski.a@pg.com

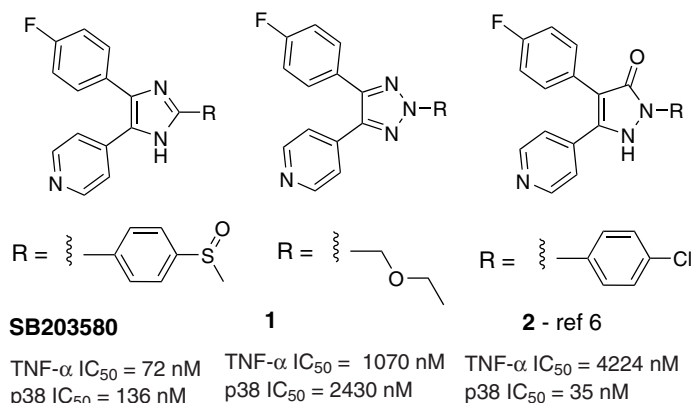
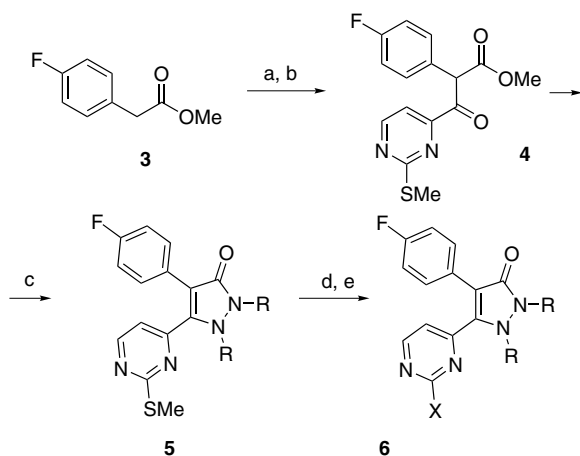


Figure 1. p38 α -kinase/TNF α synthesis inhibitors.

pyrazolones. All compounds were tested for the inhibition of TNF- α production using lipopolysaccharide (LPS) stimulated human monocytic cells (THP-1).¹¹

The synthesis of the first compounds in this series was based on the addition of alkyl hydrazines to β -ketoester **4**. Coupling of methyl-4-fluorophenylacetate (**3**), (Scheme 1) with 2-thiomethylpyrimidine-4-carboxaldehyde as described by Smith et al.¹⁰ followed by chromium oxidation provides β -ketoester **4**. Addition of symmetrically substituted hydrazines to β -ketoester **4** gives the core pyrazolone ring system **5**. Further functionalization of the pyrimidine ring was achieved via an oxidation–nucleophilic substitution reaction sequence, using sodium phenoxide, leading to pyrazolone **6a**.

In general, amino substitution at the pyrimidine ring led to more active compounds than with phenoxy analogs (this trend was also observed in the bicyclic pyrazolone series—see Refs. 7,8). An attempt to increase solubility by replacement of the benzyl amino substituent with amino-pyridine ring system led to decrease of activity (compare **6e** vs **6f**, **6g**, **6h**). Increasing the size of the substitution on the ring nitrogens of the pyrazolone



Scheme 1. Reagents and conditions: (a) LDA, THF, -78°C , 2-methylsulfanyl-pyrimidine-4-carbaldehyde; (b) CrO_3 , pyridine; (c) $\text{RNHNHR}\cdot\text{HCl}$, EtOH, 90°C ; (d) Oxone®, THF/MeOH/ H_2O , rt; (e) R^1NH_2 , toluene, 120°C or ArOH , NaH, THF.

Table 1. Symmetrically substituted pyrazolones

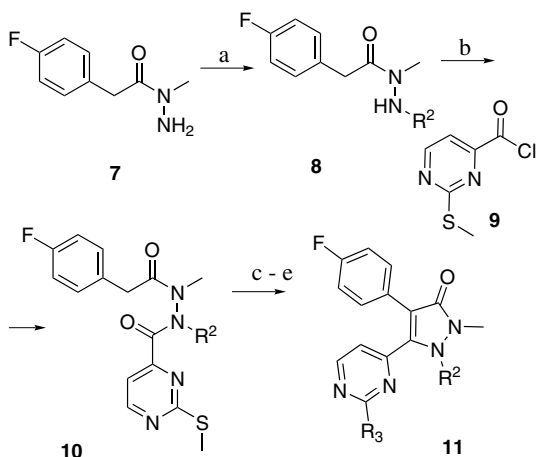
Compound	R ¹	R ²	R ³	TNF α IC ₅₀ (nM)
6a	Me	Me		288
6b	Me	Me		41
6c	Me	Me		1431
6d	Me	Me		3970
6e	Me	Me		13
6f	Me	Me		1429
6g	Me	Me		647
6h	Me	Me		>5000
6i	Et	Et		120

All chiral compounds are pure enantiomers as indicated.

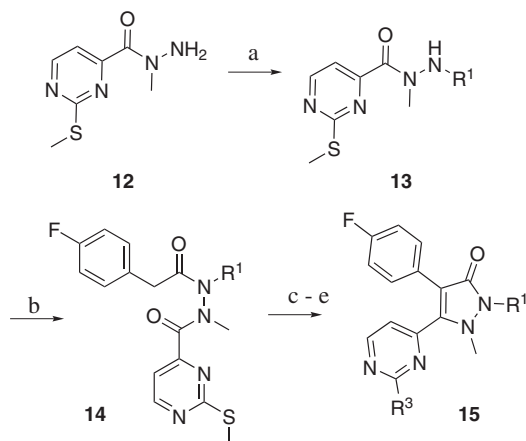
from methyl to ethyl resulted in a 10-fold loss of potency (compare **6e** vs **6i**). Isobutyl analog (**6b**) showed very good potency however is potentially metabolically unstable. All our attempts to substitute it with more metabolically stable fragments resulted in a surprising loss of activity (e.g., **6c,d**) (see Table 1).

In order to increase solubility of our compounds we decided to explore SAR around non-symmetrically substituted pyrazolones. For the synthesis of this class of compounds we applied an alternative synthetic protocol that was developed recently in our group (Scheme 2).

Hydrazone formation between acylated hydrazine **7** and an aldehyde ($R^2\text{CHO}$), followed by hydride reduction led to trisubstituted hydrazine **8**. Acylation using acid chloride **9** afforded bis-acylated hydrazine **10**. Sodium hydride mediated cyclization followed by sulfoxide formation and displacement led to the final compound **11**.



Scheme 2. Reagents and conditions: (a) $R^2\text{CHO}$, EtOH, reflux, 15 min; then NaBH_3CN , MeOH, pH 4; (b) acid chloride **9**, pyridine; (c) NaH, DMF, 0°C ; (d) *m*CPBA, DCM; (e) $R^4\text{NH}_2$, toluene + 120°C , or PhOH, NaH, THF.

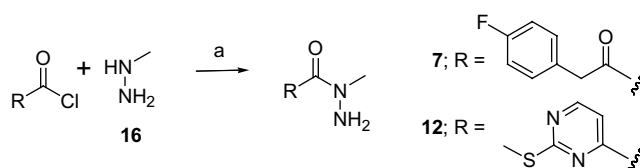


Scheme 3. Reagents and conditions: (a) $R^1\text{CHO}$, EtOH, reflux, 15 min; then NaBH_3CN , MeOH, pH 4; (b) 4-fluorophenylacetyl chloride, pyridine; (c) NaH, DMF, 0°C ; (d) *m*CPBA, DCM; (e) $R^4\text{NH}_2$, toluene + 120°C , or PhOH, NaH, THF.

A complementary, regioisomer synthesis starts with hydrazine **12**, which in an analogous synthetic sequence was transformed into pyrazolone **15** (see Scheme 3).

Syntheses of both 1,1-acyl-methyl hydrazines **7** and **12** were accomplished in one step via a highly regioselective monoacylation of methyl hydrazine¹² (see Scheme 4).

Tables 2 and 3 summarize a preliminary survey of phenoxy- and amino-pyrimidine substituents for the non-symmetrically substituted, monocyclic pyrazolones of type **11**—with R^1 substituent fixed as methyl ($R^1 = \text{Me}$) and monocyclic pyrazolones type **15**—with R^2 substituent fixed as methyl ($R^2 = \text{Me}$). In general, substitution of either methyl group with a more polar functional group increased potency (compare **6d**, **11d**,



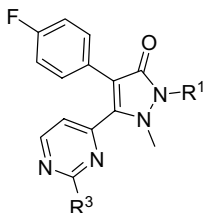
Scheme 4. Reagents and conditions: (a) DCM, -78°C .

Table 2. Non-symmetrically substituted pyrazolones **11** ($R^1 = \text{Me}$)

Compound	R^2	R^3	TNF- α IC ₅₀ (nM)
11a			1428
11b			2652
11c			924
11d			75
11e			155
11f			309

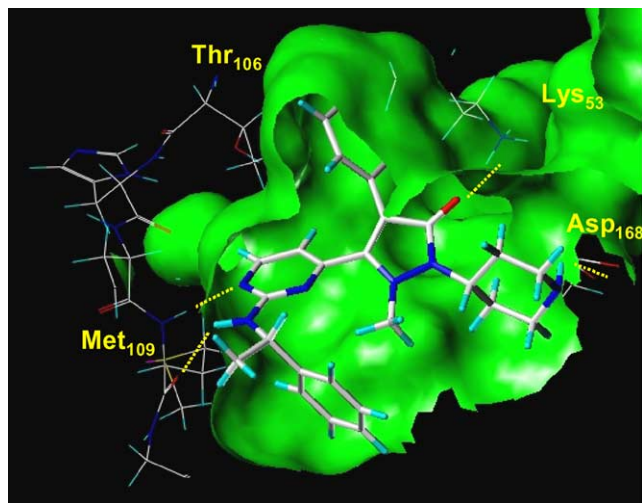
All chiral compounds are pure enantiomers as indicated.

Table 3. Non-symmetrically substituted pyrazolones **15** ($R^2 = \text{Me}$)

			
Compound	R^1	R^3	TNF- α IC ₅₀ (nM)
15a			1814
15b			1085
15c			261
15d			32
15e			15
15f			14

All chiral compounds are pure enantiomers as indicated.

15c). Presumably this could result from picking up additional polar interaction with the Asp168 carboxylate group (Figure 2).

**Figure 2.** Compound **15d** bound in the active site of mutated p38 α -kinase.**Table 4.** Pharmacokinetic properties and in vivo data of selected compounds (rat)

Compound	TNF- α IC ₅₀ (nM)	Metab ^a	Sol (mg/mL)	$t_{1/2}$ (h)	F (%)
6e	13	44	0.123	1.1	32
11d	75	0	>30.0	2.2	15
11f	309	30	0.429	ND	ND
15d	32	32	0.650	3.2	17

^a Metabolism measured as percent loss at 4 h in rat hepatocytes.

X-ray analysis of compound **15d** cocrystallized with mutated p38 kinase is presented in Figure 2.¹³ A hydrogen bond between the backbone amide N–H of Met-109 and the pyrimidine ring was observed. A second hydrogen bond was formed between the N–H of the amine substituent and the backbone carbonyl of Met-109. The pyrazolone carbonyl forms a third hydrogen bond with the Lys 53 amine group. A favorable interaction between the piperidine ring and Asp168 carboxylate group is also observed.

One of our early goals was to improve the aqueous solubility of initial leads. Unfortunately this led to compounds with lower bioavailability (Table 4). From the series of monocyclic pyrazolones only compound **6e** was found to significantly ($p < 0.05$) inhibit knee joint degeneration in the rat iodoacetate (RIA) model of osteoarthritis (dose 25 mg/kg).^{16,17}

In conclusion, we have reported the synthesis of a series of cytokine synthesis inhibitors, based on a monocyclic pyrazolone scaffold. Many of these inhibitors showed low nanomolar activity in whole cell assay (inhibition of TNF- α release from lipopolysaccharide (LPS) induced THP-1 cells). Pyrazolone **6e** was found to be orally active in rat iodoacetate (RIA) in vivo model of osteoarthritis.

Acknowledgements

We are grateful to S. Heitmeyer, K. Brown, and K. Yuellig for rat iodoacetate data; A. L. Roe, D. C. Ackley, A. M. Walter, C. R. Dietsch, and D. M. Bornes for PK and metabolic stability data, and M. Buchalova for solubility data.

We would also like to acknowledge that the X-ray data were collected at Southeast Regional Collaborative Access Team (SER-CAT) 22-ID beam line at the Advanced Photon Source, Argonne National Laboratory. Supporting institutions may be found at www.ser-cat.org/members.html. Use of the Advanced Photon Source was supported by the US Department of Energy, Office of Science, Office of Basic Energy Sciences, under Contract No. W-31-109-Eng-38.

References and notes

- For a recent review, see: Adams, J. L.; Badger, A. M.; Kumar, S.; Lee, J. C. p38 MAP Kinase: Molecular Target for the Inhibition of Pro-inflammatory Cytokines

- In *Progress in Medicinal Chemistry*; King, F. D., Oxford, A. W., Eds.; Elsevier: Amsterdam; 38, pp 1–60.
2. Badger, A. M.; Bradbeer, J. N.; Votta, B.; Lee, J. C.; Adams, J. L.; Griswold, D. E. *J. Pharmacol. Exp. Ther.* **1996**, 279, 1453.
 3. Boehm, J. C.; Adams, J. L. *Expert Opin. Ther. Pat.* **2000**, 10, 25.
 4. Jackson, P. F.; Bullington, J. L. *Curr. Top. Med. Chem.* **2002**, 2, 1011.
 5. Tullis, J. S.; VanRens, J. C.; Natchus, M. G.; Clark, M. P.; De, B.; Hsieh, L. C.; Janusz, M. J. *Bioorg. Med. Chem. Lett.* **2003**, 13, 1665.
 6. deLaszlo, S. E.; Visco, D.; Agarwal, L.; Chang, L.; Chin, J.; Croft, G.; Forsyth, A.; Fletcher, D.; Frantz, B.; Hacker, C.; Hanlon, W.; Harper, C.; Kostura, M.; Li, B.; Luell, S.; MacCoss, M.; Mantlo, N.; O'Neill, E. A.; Orevillo, C.; Pang, M.; Parson, J.; Rolando, A.; Sahly, Y.; Sidler, K.; Widmer, W. R.; O'Keefe, S. J. *Bioorg. Med. Chem. Lett.* **1998**, 8, 2689.
 7. Clark, M. P.; Laughlin, S. K.; Laufersweiler, M. J.; Bookland, R. B.; Brugel, T. A.; Golebiowski, A.; Sabat, M. P.; Townes, J. A.; VanRens, J. C.; Djung, J. F.; Natchus, M. G.; De, B.; Hsieh, L. C.; Xu, S. C.; Heitmeyer, S. A.; Brown, K. K.; Juergens, K.; Brown, K. K.; Mekel, M. J.; Taiwo, Y. O.; Janusz, M. J. *J. Med. Chem.* **2004**, 47, 2724.
 8. Laufersweiler, M. J.; Brugel, T. A.; Clark, M. P.; Golebiowski, A.; Bookland, R. G.; Laughlin, S. K.; Sabat, M. P.; Townes, J. A.; VanRens, J. C.; De, B.; Hsieh, L. C.; Heitmeyer, S. A.; Juergens, K.; Brown, K. K.; Mekel, M. J.; Walter, R. L.; Janusz, M. J. *Bioorg. Med. Chem. Lett.* **2004**, 14, 4267.
 9. Laughlin, S. K.; Clark, M. P.; Djung, J. F.; Golebiowski, A.; Brugel, T. A.; Sabat, M. P.; Bookland, R. G.; Laufersweiler, M. J.; VanRens, J. C.; Townes, J. A.; De, B.; Hsieh, L. C.; Xu, S. C.; Walter, R. L.; Mekel, M. J.; Janusz, M. J. *Bioorg. Med. Chem. Lett.*, submitted for publication.
 10. Smith, A. B., III, et al. *Synthesis* **1981**, 567.
 11. Procedure for determining IC₅₀ values of LPS-stimulated TNF- α production in human monocytic cells (THP-1): Duplicate cultures of human monocytic cells (THP-1)¹⁴ cells (2.0×10^5 /well) were incubated for 15 min in the presence or absence of various concentrations of inhibitor before the stimulation of cytokine release by the addition of lipopolysaccharide (LPS, 1 μ g/ml). The amount of TNF- α released was measured 4 h later using an ELISA (R&D Systems, Minneapolis, MN). The viability of the cells after the 4 h incubation was measured using MTS assay¹⁵ (Promega Co., Madison, WI). Standard deviation for THP-1 cellular assays was typically $\pm 30\%$ of the mean or less.
 12. Selective acetylation of methyl hydrazine was previously reported: Norton, P. P.; Shyam, S. *J. Heterocycl. Chem.* **1977**, 14, 1447.
 13. The mutated p38 α herein described is an inactivated, double mutant (S180A, Y182F) of murine p38 α . For more details see Ref. 7. The crystal structure of compound **15d** bound to mutated p38 α -kinase has been deposited in the Protein Data Bank with RCSB/PDB information is as follows: PDB Code: 1YWR; RCSB code: RCSB032009.
 14. Mohler, K. M.; Sleath, P. R.; Fitzner, J. N.; Cerretti, D. P.; Alderson, M.; Kerwar, S. S.; Torrance, D. S.; Otten-Evans, C.; Greenstreet, T.; Weerawarna, K.; Kronhelm, S. R.; Petersen, M.; Gerhart, M.; Kozlosky, C. J.; March, C. J.; Black, R. A. *Nature* **1994**, 370, 218.
 15. Bartrop, J. A.; Owen, T. C.; Cory, A. H.; Cory, J. G. *Bioorg. Med. Chem. Lett.* **1991**, 1, 611.
 16. Sprague–Dawley male rats (200–225 g) from Harlan (Oregon, WI) under anesthesia were injected in the patellar ligament region of the left leg (flexed 90° at the knee) with 20 μ L of a 10 mg/mL concentration of monosodium iodoacetate (IA) (Aldrich Chemical, Milwaukee, WI). Animals (groups of 15) were dosed for 7 days BID (~every 12 h) with the potential inhibitor (25 mg/kg) or vehicle (2.5 mL/kg). Animals were sacrificed on day 22 and the left joint was disarticulated and fixed in 10% formalin for 24–48 h prior to capturing the image. An image of the tibial cartilage surface was captured using an Optimas (Optimas, Media Cybernetics LP, Silver Springs, MA) image analysis system. Three independent observers assessed the damage in a blinded manner using a scale of 0–4 of increasing severity (0 = normal; 4 = maximum severity).
 17. Janusz, M. J.; Hookfin, E. B.; Heitmeyer, S. A.; Woessner, J. F.; Freemont, A. J.; Hoyland, J. A.; Brown, K. K.; Hsieh, L. C.; Almstead, N. G.; De, B.; Natchus, M. G.; Pikul, S.; Taiwo, Y. O. *Osteoarthr. Cartilage* **2001**, 9, 751.